

Electrochemical Detection of Dopamine in the Presence of Ascorbic Acid Using Overoxidized Polypyrrole/Graphene Modified Electrodes

Zhenjing Zhuang^{1,*,&}, Jianyong Li^{1,&}, Ruian Xu¹, Dan Xiao²

¹ Institute of Molecular Medicine, Huaqiao University, Fujian 362021, P.R. China.

² College of Chemical Engineering, Sichuan University, Chengdu 610065, P.R. China.

*E-mail: zhuangzhenjing@hqu.edu.cn

& equal contribution.

Received: 22 April 2011 / Accepted: 12 May 2011 / Published: 1 June 2011

Overoxidized polypyrrole/graphene modified glassy carbon electrode (PPyox/graphene/GCE) has been prepared and applied for the fabrication of dopamine sensors without the interference of ascorbic acid. Compared to bare GCE, a substantial negative shift of the anodic peak potential and dramatic increase of current signal were observed and the separations between the anodic and cathodic peaks of dopamine was obviously decreased, demonstrating that PPyox/graphene/GCE exhibited favorable electron transfer kinetics and electrocatalytic activity towards the oxidation of dopamine. Furthermore, PPyox/graphene/GCE exhibited good ability to suppress the background current from large excess ascorbic acid. The electrochemical detection of dopamine in the presence of ascorbic acid (1 mM) showed two linear ranges with a transition point at 25.0 μM . The sensor displayed a linear range of 25.0 μM –1.0 mM DA with a correlation coefficient of 0.996, a sensitivity of 0.015 $\mu\text{A}/\mu\text{M}$, and a linear range of 0.5 μM –10.0 μM DA with a correlation coefficient of 0.997, a sensitivity of 0.094 $\mu\text{A}/\mu\text{M}$. The detection limit was 0.1 μM with a signal/noise ratio of 3.

Keywords: Graphene, dopamine, electrochemical, overoxidized polypyrrole, sensor

1. INTRODUCTION

Dopamine (DA), one of the most significant catecholamine, plays a very important role in the functioning of the central nervous system, cardiovascular, renal and hormonal systems as well as in drug addiction and Parkinson's disease [1,2]. The quantification of DA becomes more and more important in clinical tests, serum and urine. DA often coexists with high concentration of ascorbic acid (100 – 1000 times) in biological samples, which results in poor selectivity and sensitivity for DA detection. Furthermore, ascorbic acid (AA) is oxidized at almost the same potential as DA [3,4],

resulting an overlapping voltammetric response for the oxidation of a mixture of DA and AA. The development of a simple and rapid method for the determination of DA with high selectivity and sensitivity is desirable for diagnostic applications.

In recent years, nanomaterials with special physical and chemical properties have been widely applied in chemosensors and biosensors [5-8]. As a new member of the family of carbon-based nanomaterials, graphene has attracted enormous interest in fundamental and applied science communities recently. Graphene exhibits unusual electronic conductivity, high specific surface area, high mechanical, thermal and chemical stabilities [9-14] that make it a suitable material for electrochemical catalysis and biosensing. The direct electro-oxidation of different electroactive species such as paracetamol [15], carbendazim [16], guanosine [17], aminophenol [18], hydrogen peroxide [19, 20], catechol [21], hydroquinone [22], explosives [23], adenine [24,25], and so on [26-35] have been explored on the graphene-based modified electrode. Recently there are also some efforts in the development of electrochemical methods for the determination of DA by using graphene-based modified electrodes [36-44], and revealed that graphene should be a kind of more advanced carbon electrode material for electrochemical sensors design.

On the other hand, as one of the most important conducting polymers, polypyrrole (PPy) have been extensively studied because of its potential application. However, the PPy film can be further overoxidized at higher potentials and lost its conductivity [45]. During overoxidation process, the doping ions were expelled from the polymer film, and oxygen containing groups such as carbonyl and carboxyl were introduced to the pyrrole unit, resulting in a cation perm-selectivity and a porous structure film [46,47]. Many reports have demonstrated that overoxidized polypyrrole (PPyox) films have widened applications of PPy films in electroanalytical chemistry for its excellent cation exchange and molecular sieve properties. The PPyox film has been used to fabricated glucose [48], alcohol [49], hydrazine [50], and DA [51-54] sensor. Furthermore, the usually PPyox-based modified electrodes have lower background currents [52,53].

In the present work, by combining the unique electronic properties of graphene with the excellent cation exchange and molecular sieve properties of PPyox films, the PPyox/graphene modified glassy carbon electrode (GCE) exhibited favorable electron transfer kinetics and electrocatalytic activity towards the oxidation of DA. Complete peak separation between DA and AA was observed at the PPyox/graphene modified GCE. Furthermore, the selective determination of DA was confirmed in an excess amount of AA at the PPyox/graphene modified GCE, and DA can be detected with good sensitivity and selectivity.

2. EXPERIMENTAL

2.1. Reagents

Graphene (NO. KNG110) was kindly provided by Xiamen Kaina Graphene Technology Corp. (Xiamen, China) and used as received. Pyrrole (98%) was purchased from Guoyao Chemical Reagent Factory (Shanghai, China) and purified by double distillation under reduced pressure (~1200 Pa).

Dopamine (DA), ascorbic acid (AA), sodium dodecyl sulphonate (SDS), potassium ferricyanide, phosphate sodium hydrogen phosphate, sodium dihydrogen phosphate were all purchased from Shanghai Jingchun Reagent Ltd. Corp. (Shanghai, China) and used without further purification. All reagents were of analytical grade or above. Deionized water was used throughout the experiments ($18.2\text{M}\Omega\text{ cm}^{-1}$), and all experiments were operated at room temperature.

2.2. Instrumentations

Scanning electron microscopy (SEM) images were recorded on a Hitachi S-4800 scanning electron microscope. The electrochemical experiments were performed with a CHI660D electrochemical workstation (Shanghai, China). All experiments were carried out by a three-electrode system with a bare glassy carbon electrode or modified glassy carbon electrode (GCE, $\phi = 3\text{ mm}$) as the working electrode, a Pt wire as the auxiliary electrode, and an Ag/AgCl with saturated KCl as the reference electrode.

2.3. Preparation of PPyox/graphene/GCE modified electrodes

GCE was polished subsequently with 0.3 and 0.05 μm alumina slurry, sonicated in water for several times, and dried under infrared lamp. 1.0 mg graphene was dispersed in 1.0 mL 0.1 M SDS aqueous solution and sonicated for 1 h to form a homogenous suspension. The graphene modified GCE (denoted as graphene/GCE) was prepared by dropping 3.0 μL of the graphene suspension on the surface of freshly polished GCE and dried under infrared lamp. Polypyrrole were electropolymerized on the graphene modified electrodes by cyclic voltammetry from 0.1 to 1 V with the scan rate 50 $\text{mV}\cdot\text{s}^{-1}$ for eight circles in a deaerated solution of 150 mM pyrrole and 50 mM NaClO_4 . The pyrrole polymerization was carried out under N_2 atmosphere at room temperature. The obtained modified electrode, denoted as PPy/graphene/GCE, was rinsed with water, and transferred to 0.5 M NaOH for electrochemical oxidation at 1.2 V for several minutes until the current decreased to 8 μA . The obtained electrode, denoted as PPyox/graphene/GCE, was gently washed with deionized water to remove any non-adsorbed species. For the sake of comparison, graphene/GCE, PPyox/GCE, and PPy/graphene/GCE were also prepared under the same conditions.

3. RESULTS AND DISCUSSION

3.1. Characterizations of PPyox/graphene/GCE

Figure 1 (yellow curve) shows a typical cyclic voltammograms (CVs) of a graphene/GCE in 0.1 M phosphate buffer solution (PBS, pH 5.6). The CVs curve shows a redox couple centered at -0.09 vs. Ag/AgCl, maybe corresponding to the redox of carboxylic acid groups [53]. However, this redox peaks disappear for the PPyox/graphene/GCE (Figure 1, red curve). We did not know the exact reason

but it might be due to the PPyox film coated on the surface of graphene/GCE. On the other hand, different background currents can also be observed for the bare GCE, graphene/GCE, and PPyox/graphene/GCE. Figure 1 also shows that the background current of the PPyox/graphene/GCE is apparently larger than that of the bare GCE (Figure 1, magenta curve). However, the background current of PPyox/graphene/GCE decreases a lot when comparing with PPy/graphene/GCE (data not shown), indicating anodic polarization at +1.2 V for 500 s maybe turn the PPy into an insulating overoxidized polypyrrole (PPyox) with a large loss of electroactivity [54]. Obviously, elimination of high background currents typical of PPy composite modified electrodes would also enhance analytical usefulness of these composite films, making lower detection limits attainable [47].

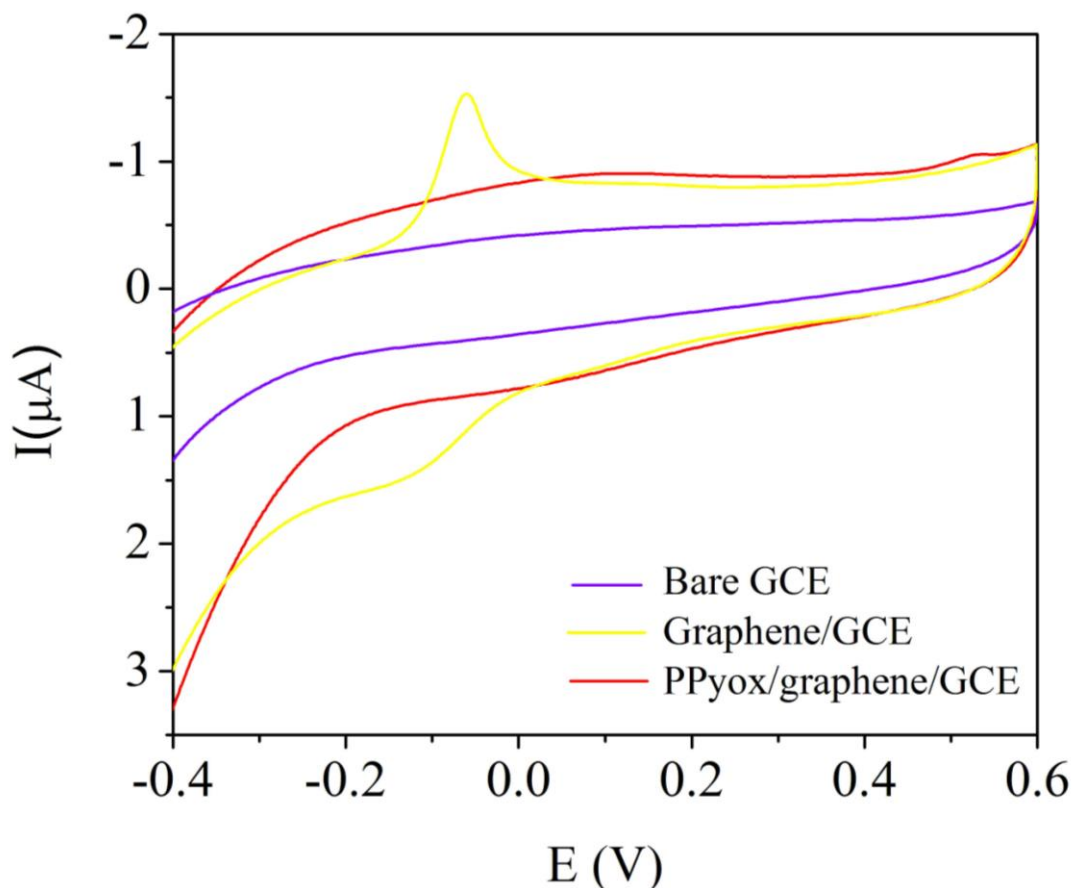


Figure 1. Cyclic voltammograms (CVs) of the graphene/GCE (yellow curve), PPyox/graphene/GCE (red curve) and the bare GCE (magenta curve) in 0.1 M PBS solution (pH 5.6). The scan rate is $50 \text{ mV} \cdot \text{s}^{-1}$.

The morphology of PPyox/graphene nanocomposite was characterized by SEM, as shown in Figure 2. It can be clearly seen that the PPyox/graphene film present a rather porous morphology consisting of flakelike structure, which may be attributed to the incorporation of graphene into the PPyox film during electropolymerization [55].

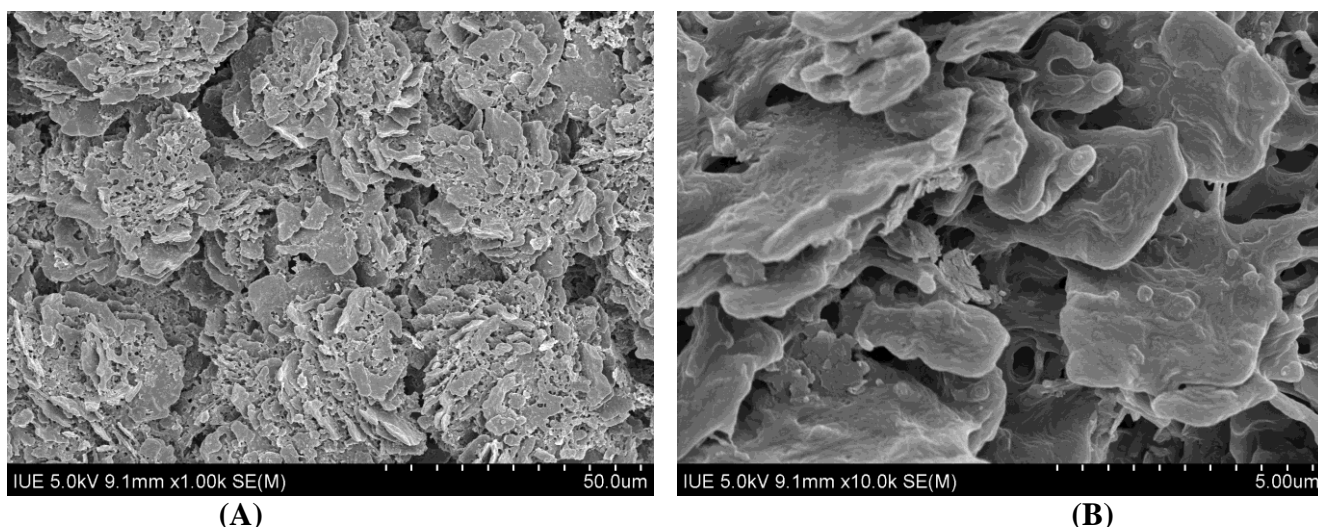


Figure 2. SEM images of PPyox/graphene composite film on GCE. (A) Magnification 1000 \times , (B) Magnification 10000 \times .

3.2. Electrochemical oxidation of DA at PPyox/graphene/GCE

Figure 3 presents the CVs of 0.1 mM DA on the bare GCE (A), PPyox/GCE (B) and PPyox/graphene/GCE (C) in 0.1 M PBS (pH 5.6), respectively. At the bare GCE, DA shows a pair of redoxwaves with the anodic and cathodic peaks at 349 mV and 164 mV, respectively. In the case of the PPyox/graphene/GCE, the corresponding oxidation peak potential is negatively shifted to 288 mV, and the peak current is approximately enhanced by 2.2 times in comparison with that of the bare GCE. For the PPyox/GCE, however, almost no voltammetric response could be observed after addition of DA. These results indicate that graphene has high electrocatalytic activity towards the oxidation of DA. The peak-to-peak separation ($\Delta E_p = E_{pa} - E_{pc}$) for the CV curves is about 30 mV at the PPyox/graphene/GCE while ΔE_p values is approximately 185 mV at the bare GCE. DA shows smaller peak-to-peak separation at the PPyox/graphene/GCE also shows that PPyox/graphene/GCE increase the electron transfer kinetics in comparison with the bare GCE.

CVs of DA at various scan rates on the PPyox/graphene/GCE were shown in Figure 4. Both the values of anodic peak current (I_{pa}) and cathodic peak current (I_{pc}) exhibit linear relationship with scan rate over the range of 49–400 $\text{mV}\cdot\text{s}^{-1}$. The linear regression equations, $I_{pa} (\mu\text{A}) = -4.1044 + 1.2373v^{1/2} (\text{mV}\cdot\text{s}^{-1})^{1/2}$ ($R=0.9977$) and $I_{pc} (\mu\text{A}) = 3.4803 - 0.7885v^{1/2} (\text{mV}\cdot\text{s}^{-1})^{1/2}$ ($R=0.9989$) were obtained, respectively (inset in Figure 4). These results imply that the electrocatalytic reaction is diffusion controlled, which is ideal for quantitative analysis in practical applications.

The effect of solution pH on the response of DA was investigated (data not shown). The anodic peak potential shifts linearly to more negative values as pH increases over a range from 4.6 to 10.6, which indicating that the redox couple of DA includes some proton transfer in the reduction and oxidation processes. According to the Nernst equation, the slope of -55.7 mV/pH unit reveals that the proportion of the electron and proton involved in the reactions is 1:1. As the DA oxidation is a two-electron process, the number of protons involved is also predicted to be two. It also can be seen that the

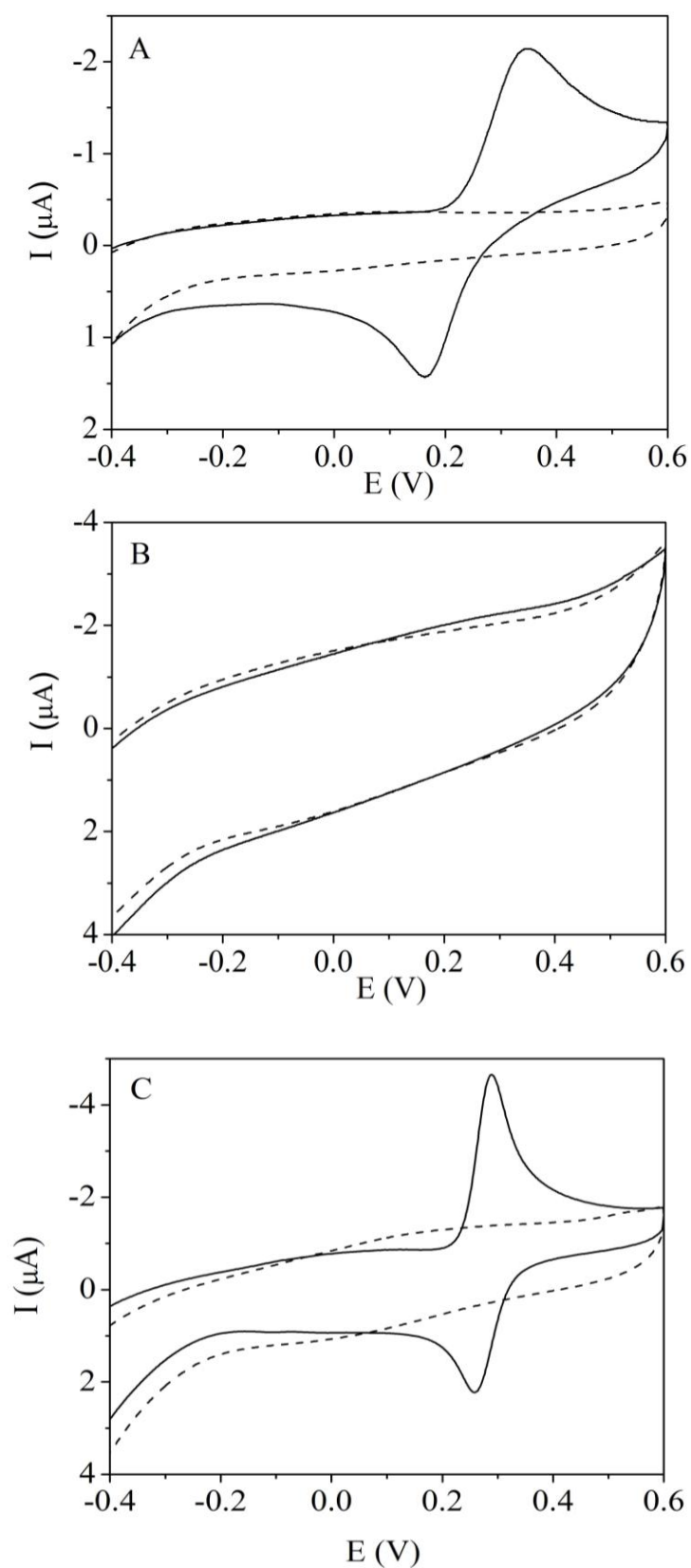


Figure 3. CVs of 0.1 mM DA at the bare GCE (A), PPyox/GCE (B) and PPyox/graphene/GCE (C) in 0.1 M PBS solution (pH 5.6). Solid and dashed curves represent the CVs with and without DA, respectively. The scan rate is $50 \text{ mV} \cdot \text{s}^{-1}$.

I_{pa} was increased with the pH value until it reached 5.6 and then decreased with the further increase in the pH value. As such, pH 5.6 was chosen for subsequent experiments.

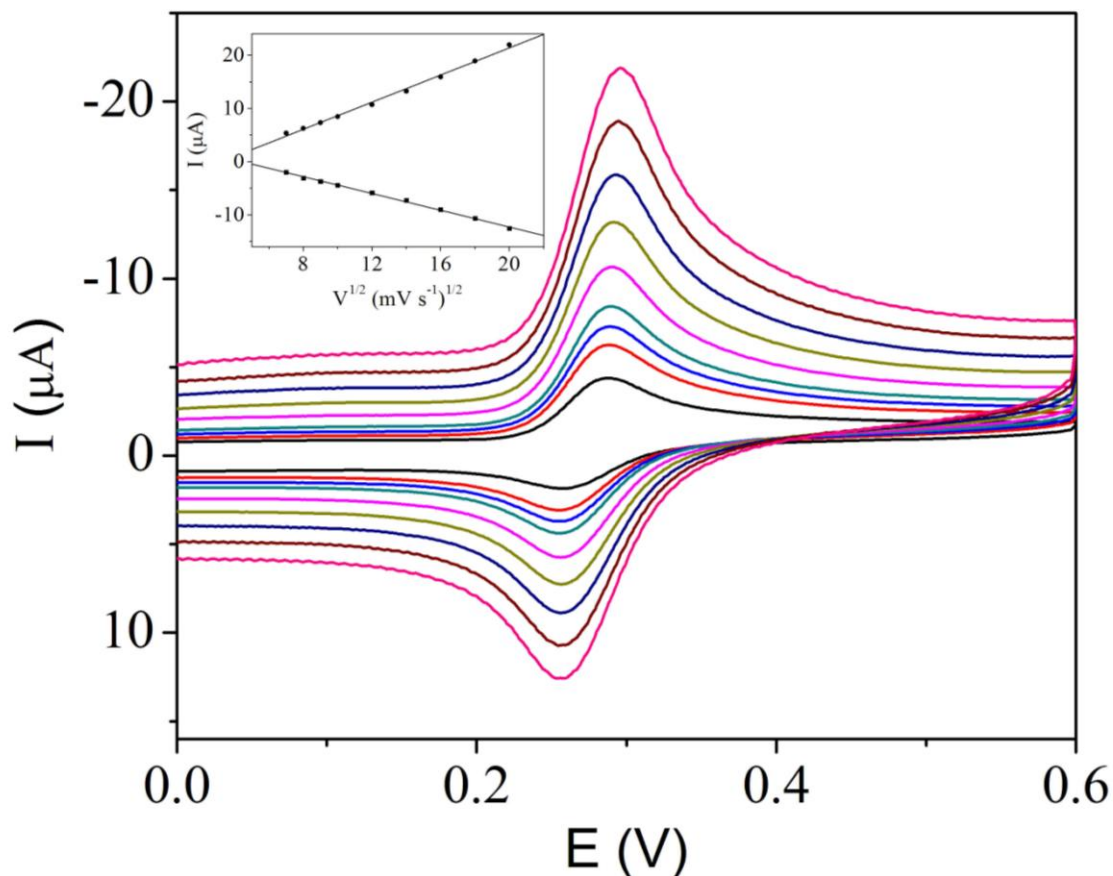


Figure 4. CVs of 0.1 mM DA at PPyox/graphene/GCE with different scan rates (49, 64, 81, 100, 144, 196, 256, 324, 400 $\text{mV}\cdot\text{s}^{-1}$) in 0.1 M PBS (pH 5.6). Inset shows the plots of peak current vs. the square root of the scan rate

3.3. Selective determination of DA

PPyox films, as mentioned before, can be regarded as negatively charged polymer films, which effectively attract the positive cation to the films and reject the diffusion of anions to the films. Figure 5 compares the CVs of a bare GCE with that of the other three modified GCEs in 50 mM $\text{K}_4\text{Fe}(\text{CN})_6$ with 0.2 M KCl at $50 \text{ mV}\cdot\text{s}^{-1}$. A well behaved reversible redox wave of ferricyanide ion can be obtained at the four electrodes. ΔE_p values of 247, 284, 150, 91 mV were observed for the bare GCE, graphene/GCE, PPy/graphene/GCE, PPyox/graphene/GCE, respectively. The smallest ΔE_p values at PPyox/graphene/GCE demonstrates that PPyox/graphene/GCE increase the electron transfer kinetics in comparison with the other three electrodes. However, the faradic current of ferricyanide ion is significantly inhibited by PPyox/graphene film at the PPyox/graphene/GCE (red curve), indicating that PPyox/graphene film is negatively charged and hinders the diffusion of ferricyanide ion toward the electrode surface.

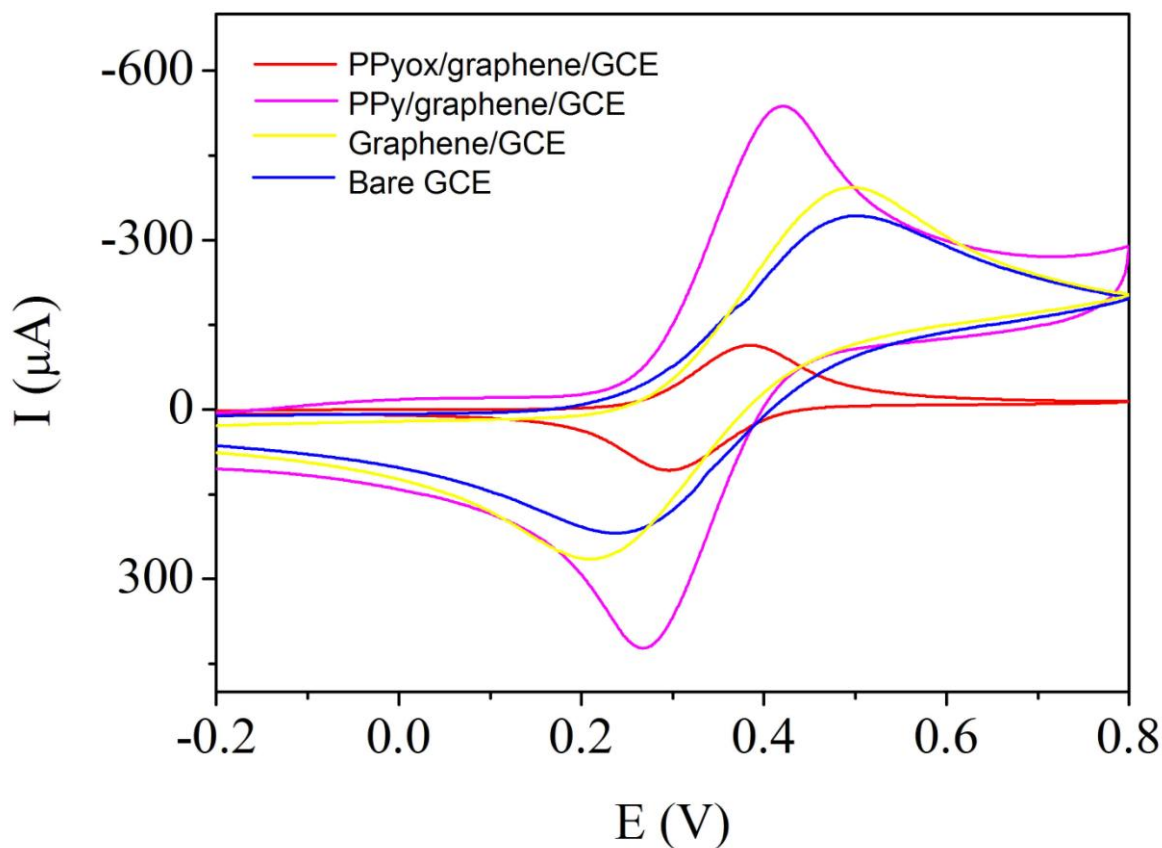


Figure 5. CVs of 50 mM $K_4Fe(CN)_6$ in 0.2 M KCl at the bare GCE (blue curve), graphene/GCE (yellow curve), PPy/graphene/GCE (magenta curve) and PPyox/graphene/GCE (red curve), respectively. The scan rate is $50 \text{ mV} \cdot \text{s}^{-1}$.

Furthermore, anions such as AA can also be rejected by PPyox/graphene films. Figure 6 shows the CVs of 0.1 mM DA at the PPyox/graphene/GCE and graphene/GCE in the presence of 1 mM AA. For the graphene/GCE, the I_{pa} of DA and AA are overlapped significantly, making the detection of DA impossible. For the PPyox/graphene/GCE, however, the oxidation peaks of AA and DA are well separated from each other for about 107 mV. As a result, the I_{pa} of DA can be readily measured in the presence of high concentration of AA. The high selectivity of the PPyox/graphene/GCE can be attributed to the negative charges on the PPyox film, which attracts positively-charged DA while repels the negatively-charged AA. Similar results can also be obtained from the PPyox-SWNTs modified GCE [53,54]. However, when comes to the CV response of DA at the PPyox/GCE, almost no voltammetric response could be observed after addition of DA in 0.1 M PBS. This may be due to the different morphology and properties of PPyox films on different substrates [46]. The selective determination of DA in the presence of AA was investigated when the concentration of DA continuously increased in the presence of 1 mM AA. As shown in Figure 7, the I_{pa} increases linearly with varying concentration of DA, while no obvious changes in the peak current of AA are observed, which demonstrate that the coexisting species AA have no interference for the determination of DA.

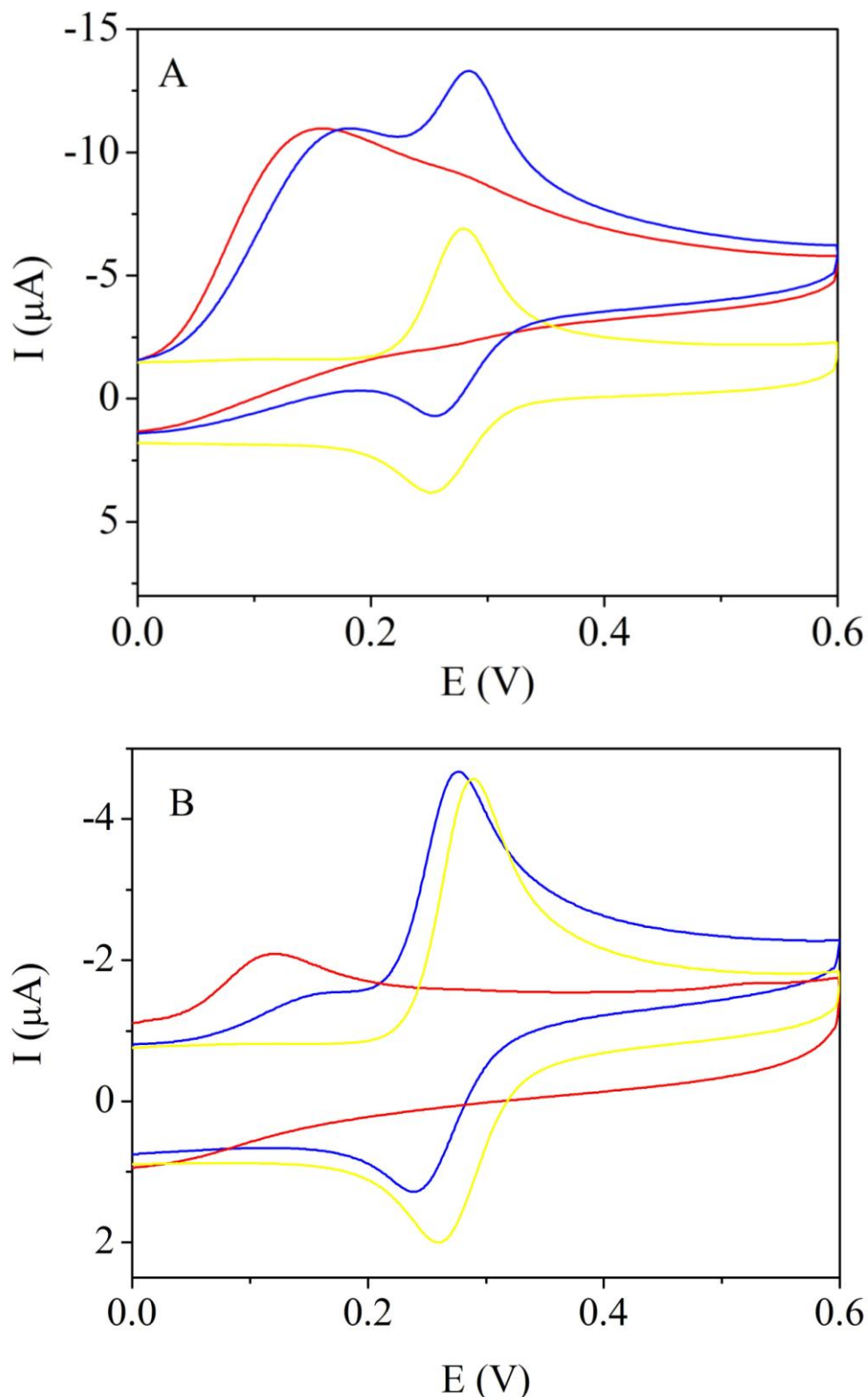


Figure 6. CVs of 0.1 mM DA (yellow curve), 1 mM AA (red curve) and 0.1 mM DA in the presence of 1 mM AA (blue curve) in 0.1 M PBS (pH 5.6) At the graphene/GCE (A) and PPyox/graphene/GCE (B), respectively. The scan rate is $50 \text{ mV} \cdot \text{s}^{-1}$.

The I_{pa} versus DA concentration curve shows two linear ranges with a transition point at 25.0 μM . The sensor displays a linear range of 25.0 μM –1.0 mM DA with a correlation coefficient of 0.996, a sensitivity of 0.015 $\mu\text{A}/\mu\text{M}$, and a linear range of 0.5 μM –10.0 μM DA with a correlation coefficient of 0.997, a sensitivity of 0.094 $\mu\text{A}/\mu\text{M}$, and a detection limit of 0.1 μM with a signal/noise ratio of 3. The two linear range phenomenon has also been observed on β -cyclodextrin/graphene nanocomposite modified electrode, and one possible origin may be the transition from monolayer adsorption state into more complicated multilayer adsorption state [41].

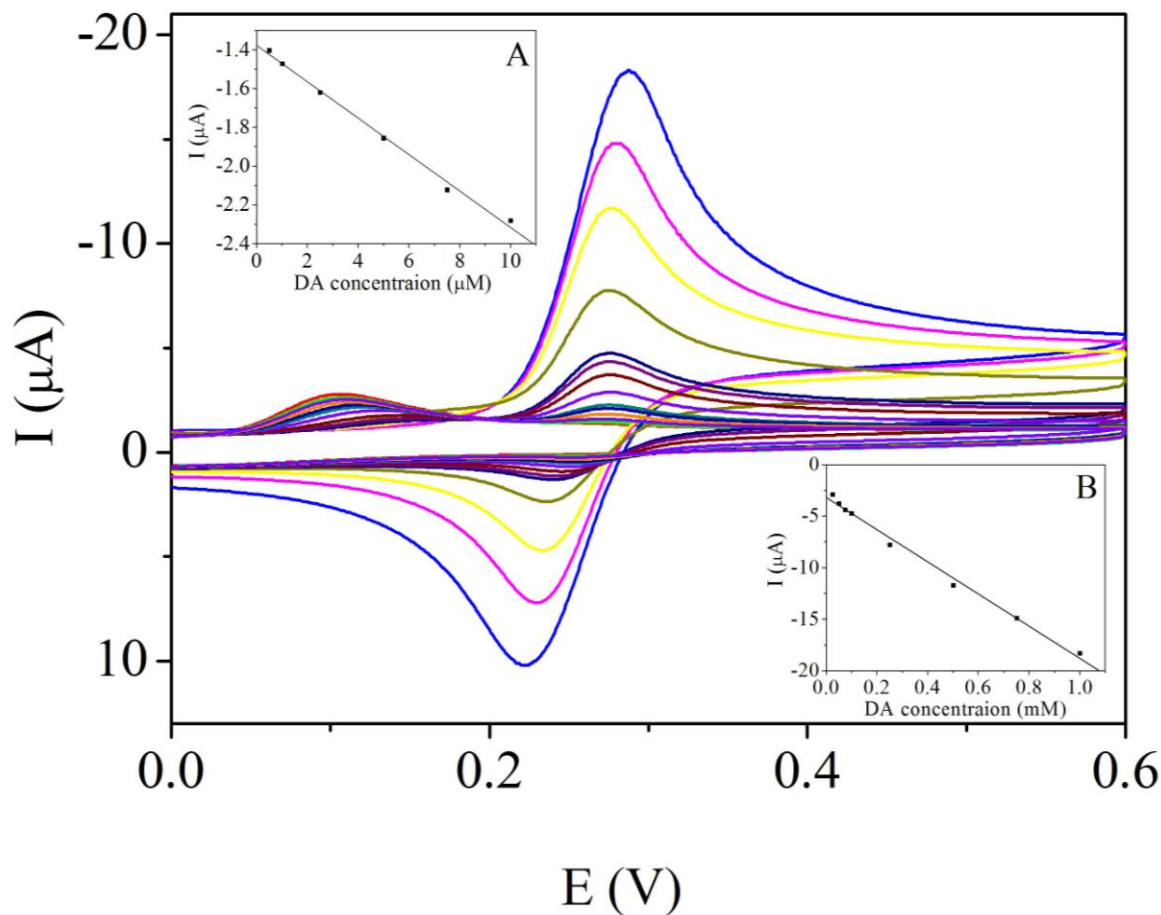


Figure 7. CVs of 0.5, 1, 2.5, 5, 7.5, 10 μM and 0.025, 0.05, 0.075, 0.1, 0.25, 0.5, 0.75, 1 mM DA at the PPyox/graphene/GCE in the presence of 1 mM AA. Insets of (A) and (B) show the relation between I_{pa} and DA concentration in the linear ranges. CVs were carried out at a scan rate of 50 $\text{mV}\cdot\text{s}^{-1}$.

It is worth noting that the sensitivity of our present DA sensor over the range of 0.5 μM –10.0 μM is largely improved than that of the previously reported work using grapheme [39-41] and the detection limit is better than the previous literature report [39,40], which may attribute to the fact that PPyox/graphene film can greatly increase their electrocatalytic active sites and promote the electron transfer in the oxidation of DA.

3.4. Stability of PPyox/graphene/GCE

The reproducibility and stability of the sensor was evaluated. Three PPyox/graphene/GCEs were made and their CVs responses to DA were investigated. The relative standard deviation (RSD) of sensitivity to DA was 4.30 % over the range of 25.0 μM –1.0 mM DA, and 4.89% over the range of 0.5 μM –10.0 μM , confirming that the fabrication method was highly reproducible. Three successive measurements of 0.1 mM and 5 μM DA on a PPyox/graphene/GCE yielded a RSD of 1.63 % and 2.04% respectively, demonstrating that the sensor was stable. The good reproducibility and excellent stability of the PPyox/graphene/GCE may be attributed to the stability of graphene and the protecting effect of PPyox film against the desorption of graphene from GCE surface.

4. CONCLUSIONS

This paper reports the fabrication, characterization and practical applications of PPyox/graphene composite film modified glassy carbon electrode. The good electronic conductivity and electrocatalytic activity of immobilized graphene combined with the selective feature of PPyox exhibited superior sensitivity and selectivity towards the oxidation of DA in the presence of AA. Furthermore, PPyox could be used as a template to immobilize graphene, which made the sensor exhibit good reproducibility and excellent stability. These favorable features of such a modified electrode offer great promise for its sensing applications, and more relative works are in progress.

ACKNOWLEDGEMENTS

The authors are grateful to the financial support from Huaqiao University, China (Research Foundation for Advanced Talents, No. 08BS413) and the Fundamental Research Funds for the Central Universities (No. JB-JD10005). This work is also supported by the funds from Fujian Graduate Education and Innovation Base of Biomedical Engineering (No. 06070205).

References

1. M. L. A. V. Heien, A. S. Khan, J. L. Ariansen, J. F. Cheer, P. E. M. Phillips, K. M. Wassum and R. M. Wightman, *Proc. Natl. Acad. Sci.*, 102 (2005) 10023.
2. R. M. Wightman, L. J. May and A. C. Michael, *Anal. Chem.*, 60 (1988) 769A.
3. Y. Liu, J. Huang, H. Hou and T. You, *Electrochem. Commun.*, 10 (2008) 1431.
4. S. S. shankar, B.E. K. Swamy, U. Chandra, J.G.Manjunatha and B.S. Sherigara, *Int. J. Electrochem. Sci.*, 4 (2009) 592.
5. Z. Zhuang, X. Su, H. Yuan, Q. Sun, D. Xiao and M. M. F. Choi, *Analyst*, 133 (2008) 126.
6. Z. Zhuang, X. Su, B. Zheng, H. Yuan, Q. Sun and D. Xiao, *Sensor Lett.*, 5 (2007) 559.
7. X. Su, Z. Zhuang, B. Lv and D. Xiao, *Sensor Lett.*, 5 (2007) 578.
8. Z. Xu, Q. Yue, Z. Zhuang and D. Xiao, *Microchim. Acta*, 164 (2009) 387.
9. D. Li and R. B. Kaner, *Science*, 320 (2008) 1170.
10. R. M. Westervelt, *Science*, 320 (2008) 324.

11. D. Li, M. B. Müller, S. Gilje, R. B. Kaner, G. G. Wallace, *Nature Nanotech.*, 3 (2008) 101.
12. M. Pumera, *Chem. Soc. Rev.*, 39 (2010) 4146.
13. M. Pumera, *Chem. Rec.*, 9 (2009) 211.
14. C. L. Scott, G. Zhao and M. Pumera, *Electrochem. Commun.*, 12 (2010) 1788.
15. X. Kang, J. Wang, H. Wu, J. Liu, I. A. Aksay and Y. Lin, *Talanta*, 81 (2010) 754.
16. Y. Guo, S. Guo, J. Li, E. Wang and S. Dong, *Talanta*, in press.
17. H. Yin, Y. Zhou, Q. Ma, S. Ai, Q. Chen and L. Zhu, *Talanta*, 82 (2010) 1193.
18. H. Yin, Q. Ma, Y. Zhou, S. Ai and L. Zhu, *Electrochim. Acta*, 55 (2010) 7102.
19. Y. Zhang, X. Sun, L. Zhu, H. Shen and N. Jia, *Electrochim. Acta*, 56 (2011) 1239.
20. W.-J. Lin, C.-S. Liao, J.-H. Jhang and Y.-C. Tsai, *Electrochem. Commun.*, 11 (2009) 2153.
21. H. Yin, Q. Zhang, Y. Zhou, Q. Ma, T. Liu, L. Zhu and S. Ai, *Electrochim. Acta*, in press.
22. J. Li, C.-Y. Liu and C. Cheng, *Electrochim. Acta*, in press
23. C. X. Guo, Y. Lei, C and M. Li, *Electroanalysis* 22 (2010) 1.
24. C. Shan, H. Yang, D. Han, Q. Zhang, A. Ivaska and L. Niu, *Biosens. Bioelectron.*, 25 (2010) 1504.
25. H. Yin, Y. Zhou, Q. Ma, S. Ai, P. Ju, L. Zhu and L. Lu, *Process Biochemistry*, 45 (2010) 1707.
26. J. Li, S. Guo, Y. Zhai and E. Wang, *Anal. Chim. Acta*, 649 (2009) 196.
27. J. Gong, T. Zhou, D. Song and L. Zhang, *Sens. Actuators B*, 150 (2010) 491.
28. J. Li, J. Chen, X.-L. Zhang, C.-H. Lu and H.-H. Yang, *Talanta*, 83 (2010) 553.
29. Y. Wan, Y. Wang, J. Wu and D. Zhang, *Anal. Chem.*, In press.
30. Z. Wang, X. Zhou, J. Zhang, F. Boey and H. Zhang, *J. Phys. Chem. C*, 113 (2009) 14071.
31. Q. Wei, K. Mao, D. Wu, Y. Dai, J. Yang, B. Du, M. Yang and H. Li, *Sens. Actuators B*, 149 (2010) 314.
32. B. Su, J. Tang, J. Huang, H. Yang, B. Qiu, G. Chen and D. Tang, *Electroanalysis*, 22 (2010) 2720.
33. S. Yang, B. Xu, J. Zhang, X. Huang, J. Ye and C. Yu, *J. Phys. Chem. C*, 114 (2010) 4389.
34. X. Xie, K. Zhao, X. Xu, W. Zhao, S. Liu, Z. i Zhu, M. Li, Z. Shi and Y. Shao, *J. Phys. Chem. C*, 114 (2010) 14243.
35. L. Zhang, Y. Li, L. Zhang, D.-W. Li, D. Karpuzov and Y.-T. Long, *Int. J. Electrochem. Sci.*, 6 (2011) 819.
36. D. Han, T. Han, C. Shan, A. Ivaska and L. Niu, *Electroanalysis*, 22 (2010) 2001.
37. M. Pumera, A. Ambrosi, A. Bonanni, E. L. K. Chng and H. L. Poh, *TrAC Trends Anal. Chem.*, 29 (2010) 954.
38. M. Zhou, Y. Zhai and S. Dong, *Anal. Chem.*, 81 (2009) 5603.
39. Y.-R. Kim, S. Bong, Y.-J. Kang, Y. Yang, R. K. Mahajan, J. S. Kim and H. Kim, *Biosens. Bioelectron.*, 25 (2010) 2366.
40. Y. Fan, H.-T. Lu, J.H.Liu, C.-P. Yang, Q.-S. Jing, Y.-X. Zhang, X.-K. Yang and K.-J. Huang. *Colloids Surf. B*, 83 (2011) 78.
41. L. Tan, K.-G. Zhou, Y.-H. Zhang, H.-X. Wang, X.-D. Wang, Y.-F. Guo and H.-L. Zhang, *Electrochem. Commun.*, 12 (2010) 557.
42. F. Li, J. Chai, H. Yang, D. Han and L. Niu, *Talanta*, 81 (2010) 1063.
43. S. Guo, D. Wen, Y. Zhai, S. Dong and E. Wang, *ACS NANO*, 4 (2010) 3959.
44. Y. Guo, S. Guo, J. Ren, Y. Zhai, S. Dong and E. Wang, *ACS NANO*, 4 (2010) 4001.
45. J. Li and X.-Q. Lin, *Anal. Chim. Acta*, 596 (2007) 222.
46. A. Witkowski and A. Brajter-Toth, *Anal. Chem.*, 64 (1992) 635.
47. A. Witkowski, M. S. Freund and A. Brajter-Toth, *Anal. Chem.*, 63 (1991) 622.
48. P.J.H.J. van OS, A. Bult and W.P. van Bennekom, *Anal. Chim. Acta*, 305 (1995) 18.
49. D. Carelli, D. Centonze, A. D. Gigli, M. Quinto and P. G. Zambonin, *Anal. Chim. Acta*, 565 (2006) 27.
50. M. R. Majidi, A. Jouyban and K. Asadpour-Zeynali, *Electrochim. Acta*, 52 (2007) 6248.
51. X. Tu, Q. Xie, S. Jiang and S. Yao, *Biosens. Bioelectron.*, 22 (2007) 2819.
52. K. Pihel, Q. D. Walker and R. M. Wightman, *Anal. Chem.*, 68 (1996) 2084.

53. J.Wen, L. Zhou, L. Jin, X. Cao and B.-C. Ye, *J. Chromatogr. B*, 877 (2009) 1793.
54. Y. Li, P. Wang, L. Wang and X. Lin, *Biosens. Bioelectron.*, 22 (2007) 3120.
55. D. Du, X. Ye, J. Cai, J. Liu and A. Zhang, *Biosens. Bioelectron.*, 25 (2010) 2503.